http://dx.doi.org/10.5012/bkcs.2012.33.10.3378

Fabrication of a Superhydrophobic Surface with Adjustable Hydrophobicity and Adhesivity Based on a Silica Nanotube Array

Jaeeun Yu[†,‡] and Sang Jun Son[†,*]

[†]*Department of Chemistry, Gachon University, Seongnam, Gyeonggi 461-701, Korea.* [*]*E-mail: sjson@gachon.ac.kr*
[‡]*Department of Chemistry, Seoul National University, Seoul 151-747, Korea*
Received July 24, 2012, Accepted July 25, 2012

A superhydrophobic surface with a water contact angle > 150° has attracted great interest from both fundamental and practical aspects. In this study, we demonstrated that hydrophobicity of a silica nanotube (SNT) array can be easily controlled by the SNT aspect ratio. In addition, the adhesive and anti-adhesive properties were controlled without modifying the hydrophobic surface. Various silica structures on a polydimethylsiloxane substrate were prepared using the desired alumina template. Bundle-arrayed and bowl-arrayed silica surfaces exhibited extraordinary superhydrophobicity due to the large frontal surface area and hierarchical micro/nanostructure. As the strategy used in this study is biocompatible and a wide range of hydrophobicities are capable of being controlled by the SNT aspect ratio, a hydrophobic surface composed of an SNT array could be an attractive candidate for bioapplications, such as cell and protein chips.

Key Words : Silica nanotube, Superhydrophobicity, Wettability, Nanoarray, Biochip

Introduction

Superhydrophobic surfaces with high adhesive force offer particular advantages to completely transport water microdroplets.[1-3] Superhydrophobic surfaces, with water contact angles (CAs) > 150°, avoid the wetting problem.[4-8] A microdroplet on this surface usually takes a quasi-spherical shape and dramatically lowers the contact area between the droplet and solid surface, which greatly reduces possible liquid deposition. In addition, the strong adhesive property of the surface holds the microdroplet accurately in place without any sliding or rolling. A superhydrophobic surface with high adhesive force can be used for reversibly oriented transport of superparamagnetic microliter-sized liquid droplets with no lost volume in alternating magnetic fields, which is of great significance for innovative design of open microfluidic devices.[9]

Besides applications for innovative devices and anti-contamination coatings, an emerging area in which hydrophobic surfaces play a key role is biomedicine, such as protein and cell chips. For example, a wide range of hydrophobicities is required to control cell adhesion, cell growth, and cell mobility on a cell chip.[10,11] Biocompatibility must also be considered for bioapplications. A superhydrophobic surface is generally prepared by a combination of lowering surface energy and enhancing surface roughness.[12] Although many hydrophobic surfaces made of various materials including polymers and inorganic nanoparticles have been successfully developed,[13,14] they still leave room for improvement in terms of biocompatibility and capability of a wide range of hydrophobicities to be used as bioapplications. In this aspect, silica material could be an attractive candidate for fabricating the hydrophobic surface because of its biocompatibility and chemical stability. Fabricating a hydrophobic surface composed of silica material has been attempted by spreading silica nanoparticles on a substrate[15,16] or by a modifying hydrophobic silanization.[17-19] However, the range of hydrophobicities capable of being controlled by a single approach is still limited.

In this study, we fabricated a hydrophobic surface based on silica nanotube (SNT) arrays without a fluorinated carbon film coating and investigated the hydrophobicity depending on the secondary nano/micro structure formed by various SNT arrays with different aspect ratios. Figure 1 is a schematic diagram for preparing the SNT arrays on a polydimethylsiloxane (PDMS) surface. First, SNTs were prepared using template synthesis and nanoporous anodic aluminum oxide (AAO). After the PDMS layer was formed on the resulting silica-coated AAO templates, the remaining backside aluminum layer and alumina template were dissolved sequentially in aqueous $HgCl_2$ and H_3PO_4 solutions, respectively. SNT arrays on PDMS were obtained by washing with deionized water and drying in air at room temperature. Various SNT arrays composed of SNTs with different aspect ratios were prepared and their CA values were measured. In addition, superhydrophobic silica nanostructures with either strong adhesive force or anti-adhesive force were demonstrated.

Experimental

Materials. Silicon tetrachloride ($SiCl_4$, 99.8%, Acros Organics, Geel, Belgium), perchloric acid (70%, DC Chemical, Midland MI, USA), mercury(II) chloride (99.5%, Daejung Chemical, Daejung, China), hexane (95%, J.T. Baker, Phillipsburg, PA, USA) were used as supplied without further purification. Aluminum foil (99.99%) was purchased from Alfa Aesar (Ward Hill, MA, USA). PDMS elastomer

kits (Sylgard 184) were purchased from Dow Corning (Midland, MI, USA).

Preparation of Silica-Coated AAO Templates. AAO templates were prepared by two-step anodization according to the literature,[20,21] except that only one side of the Al plate was anodized and the other side was protected with silicone rubber. Preannealed aluminum foil (0.25 mm thick) was degreased in acetone and then electropolished with perchloric acid and ethanol (v/v 1:5) at 15 V and 5 °C. The anodization was carried out at 40 V and 10 °C. The irregular oxide film obtained from the first step anodization was etched away in a mixed solution of chromic acid and phosphoric acid, and the final oxide film was then prepared by a second anodization. Pores were widened in phosphoric acid solution (5 wt %) at 30 °C.

Silica-coated alumina templates were obtained by the surface sol-gel method, as reported previously.[22,23] Briefly, the AAO template was dipped in $SiCl_4$, rinsed with hexane, immersed in a mixture of hexane and methanol, and then rinsed with ethanol. After drying with N_2 gas, the templates were immersed in water to finish the reaction. Four deposition cycles were performed in this study.

Fabrication of Silica Structures on a PDMS Substrate. Silica structures on PDMS were fabricated according to Figure 1. The resulting silica-coated AAO templates were placed on a clean glass plate with the anodized side up. A prepolymer of PDMS was poured onto the plate and solidified at 70 °C for 1 h. Thus, the smooth PDMS film was formed with a 2 mm thickness. After forming the PDMS, the remaining back-side aluminum layer was removed by dipping in an aqueous solution of mercuric chloride. The alumina template was then selectively dissolved in 25 wt % phosphoric acid in water/methanol (95% v/v). The silica structures on PDMS were obtained by washing with deionized water and drying in air at room temperature. A slight change in washing and drying steps would result in different morphologies of the silica structures. The morphology of the silica nano- and micro-structures on PDMS can be controlled using the desired alumina templates.

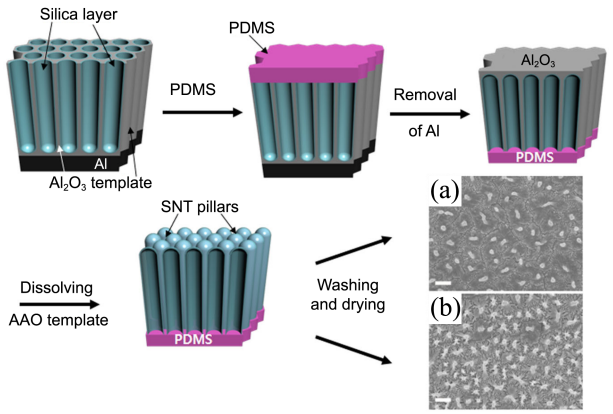

Figure 1. Schematic diagram for the preparation of silica structures on polydimethylsiloxane (PDMS). Inset images are scanning electron micrographs of silica nanobundle structures obtained from the same alumina template, but followed by different drying conditions; (a) hydrophilic and (b) hydrophobic. Scale bars, 1 μm.

Measurements. The morphological characterization of the samples was examined by field emission scanning electron microscopy (JEOL JSM-6700F and JSM-7500F; Tokyo, Japan). Water CAs were measured on a CA system (contact angle analyzer, Surface Electro Optics, Suwon, Korea; Phoenix 150/300) at ambient temperature. Water droplets (5.0 μL) were dropped carefully onto the surface of samples. The average CA values were obtained by measuring four different positions within the same sample.

Results and Discussion

Twenty nm diameter silica-coated alumina templates of various lengths were prepared. The silica nanostructures supported on continuous PDMS were prepared by removing the aluminum plate and AAO, followed by washing with deionized water and drying in air. Figure 2 shows the SEM images of the resulting silica nanostructures fabricated on PDMS. Silica nanobundle structures were obtained instead of nanopillar structures. As reported previosuly,[24,25] this result can be explained by immersion capillary forces present between the silica nanopillars during evaporation of a liquid. As the contact line of a liquid continues to recede to the root region of the nanopillar, surface tension around the contact lines produces a net attractive force between the nanopillars. As a result, silica nanopillars combine together

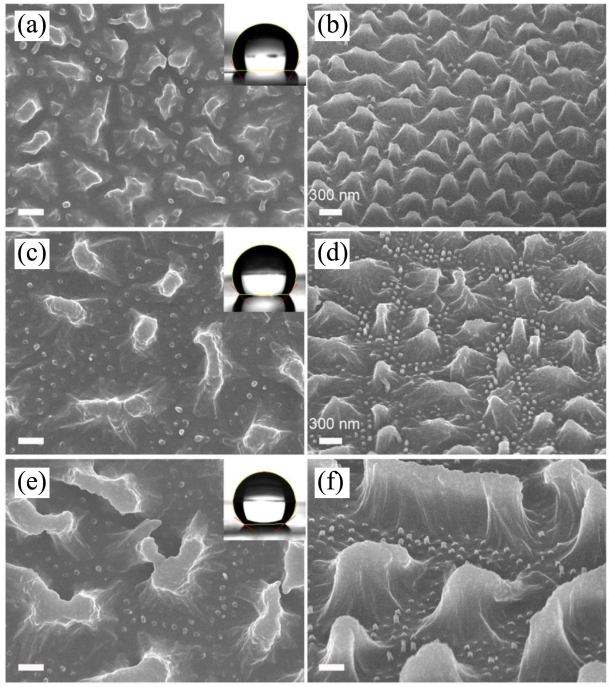

Figure 2. Scanning electron micrographic images of the silica nanotube (SNT) nanobundle structures obtained from the 200-nm alumina template (a, b); 350-nm alumina template (c, d); and 500-nm alumina template (e, f). panels b, d, and f show a 40° view of the silica nanostructures on the polydimethylsiloxane (PDMS) surface. Inset images are the shape of a water drop on the silica nanobundle-arrayed structures on PDMS, indicating their hydrophobicity. Scale bars, 200 nm, if not specified.

and form a bundle-like array.

Surprisingly, the silica nanobundle structures showed hydrophobic properties without any surface modification to decrease the surface energy (insets in Fig. 2). The CAs of the silica nanobundle structures were 122.2° (± 3.2°), 132.9° (± 1.5°), and 145.6° (± 2.4°) for those array structures obtained from 200-nm, 350-nm, and 500-nm silica-coated AAO templates, respectively. As the length of the alumina template determined the height of the silica nanostructures, the longer silica nanopillars become more flexible; thus, producing the larger bundle arrays (Fig. 2(b), 2(d), and 2(f)). It was noticeable that the apparent CA increased gradually with increasing height. This height-dependent hydrophobicity was attributed to the increasing frontal surface area of the silica layer with nanobundle-array surface morphology.

A control experiment was carried out with a glass slide as the supporter. Four-cycles of surface sol-gel were performed on the glass as with the silica-coated alumina template, and the CA was measured as 30° (Fig. 3(a)). In contrast, water droplets on the silica nanobundle-array structures showed hydrophobic behavior (insets in Fig. 2 and 3(b)), suggesting that a silica material with well-ordered nanostructures showed a hydrophobic CA although the silica layer generated by the sol-gel method was hydrophilic. In addition, the Wenzel model applies to the silica nanobundle structures, in which the droplet is able to wet the surface. Figure 3(c) and 3(d) show the behavior of the water droplet when the silica nanobundle-array on the PDMS substrate was tilted or turned upside down. It was noted that the silica nanobundle structures could hold water droplets through a strong adhesive force.

The silica nanobundle structure supported on PDMS (AAO length: 500 nm, diameter: 20 nm) was studied with X-ray photoelectron spectroscopy (XPS). The result revealed that no other particular elements were found in the silica structures, except Si, O, and C (Fig. 3(e)). The values were observed at 532.4 eV for O 1s, 285 eV for C 1s, 153 eV for Si 2s, and 102-103 eV for Si 2p, which agreed with literature values.[26] The XPS measurement of a control sample was also examined using the opposite side of the supporter, which was bare PDMS. Compared to the control analysis, the carbon peak intensity of the silica array decreased somewhat, and the oxygen peak intensity increased. The Si:C:O atomic ratio changed from 31:43:26 for the bare PDMS to 30:38:32 for the silica patterned side.

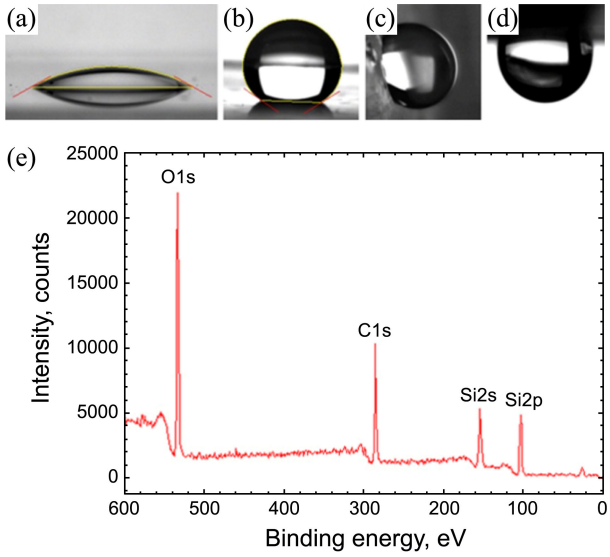

Figure 3. Micrographic pictures of a droplet on a flat surface with the silica layer (a) and silica nanobundle structures fabricated on polydimethylsiloxane (PDMS) (b). Behavior of a water droplet on nanobundle-arrayed surface with tilt angles of 80° (c) and 180° (d), respectively. (e) X-ray photoelectron spectroscopy (XPS) spectrum of silica nanobundle structures on PDMS.

It is believed that the hydrophilic interactions between the silica nanopillars played an important role to determine sample morphologies using this strategy. To investigate this factor, experimental steps were changed slightly; the resulting substrate after removing of alumina template was washed with deionized water, ethanol, acetone, and hexane, sequentially and dried in air at room temperature. Silica-coated AAO templates of 500-nm length and 20-nm diameter were used for this experiment. The result demonstrated that the interval between the silica bundles could be modulated by simply changing the washing solvent. Because hexane is a hydrophobic and volatile solvent, the drying time was shortened. Therefore, this resulted in the formation of smaller nanobundles, consisting of a smaller number of nanopillars, and eventually the fabrication of a more compact silica nanobundle structure. The width interval decreased from 1.09 (± 0.27) μm to 0.84 (± 0.20) μm, as seen in the SEM images of Figure 1. This condition, which we called the hydrophobic drying condition, can be practically applied to longer silica array structures.

Ordered silica structures on PDMS substrate were hardly observed as the length of silica-coated alumina templates increased to > 1 μm. Silica microstructures obtained from the 12 μm long 40 nm in diameter template presented a relatively irregular microstructure (Fig. 4(a)). However, an ordered silica microstructure can be prepared using the hydrophobic drying condition. Figure 4(b)-(d) shows SEM images of a highly ordered silica microbundle array on PDMS. This result clearly indicates that silica structures can be determined by drying conditions and that the resulting structures were significantly different although they were prepared from the same templates. Silica microbundle structures (inset in Fig. 4(b)) showed hydrophobic and adhesive properties with a CA of 146.2° (± 0.3°), similar to the silica nanobundle structures (inset in Fig. 3(b)). Even though the height of the silica bundle array increased, the surface did not reach a superhydrophobic state (150°); this is another example where the transition from a hydrophobic to a superhydrophobic surface might be affected by the adhesive force of the surface.[27] It is notable that disordered silica microstructures (Fig. 4(a)) also showed hydrophobicity with a CA of 136.2° (± 1.2°). This property is mainly attributed to the great frontal surface area with the arrayed surface, although the structures were not highly ordered.

Additionally, silica structures on a PDMS supporter with

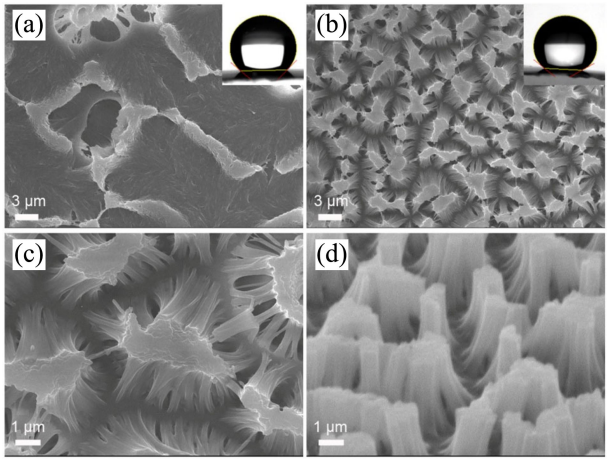

Figure 4. (a) Top-viewed scanning electron micrograph (SEM) image of the disordered silica microstructure obtained under the hydrophilic drying condition; (b-d) SEM images of silica microbundle structure fabricated on polydimethylsiloxane (PDMS) using a 40-nm diameter and 12-μm long template. Top-viewed (b, c) and 40° tilted (d) images of highly ordered silica microbundle structure obtained by washing under the hydrophobic drying condition. Inset images show the shapes of the water drop on the silica structures fabricated on the PDMS substrate, which demonstrate their hydrophobic behavior.

superhydrophobic and anti-adhesive properties were prepared successfully. An alumina template of 12 μm in length and 20 nm in diameter was used for fabrication. As described above, no such ordered-structure was found on the PDMS surface, which was obtained under the hydrophilic drying condition. A silica microbowl-array structure was fabricated using the hydrophobic drying condition. Figure 5 shows SEM images of the resulting bowl-like ordered structures at different magnifications. Interestingly, the hierarchical microstructures took on bowl-like structures with an average diameter of approximately 5 μm (Fig. 5(a), (b), and 5(d)), and each bowl-like unit has rough inner walls composed of 12-μm long nanopillars, as shown in Figure 5(c). Our silica hierarchical bowl-like structure demonstrated a 153.4° CA (inset in Fig. 5(a)), indicating its superhydrophobicity without any hydrophobic surface modification. The Cassie-Baxter model applies to the surface, where a self-cleaning property was observed like lotus leaves.[28] A droplet easily rolled off the surface, revealing that the adhesive force of the silica microbowl structure was small. This ordered microbowl array was mainly composed of air, which eventually lead to a strong reduction or elimination of CA hysteresis. Due to the morphology of the hierarchical micro/nanostructures, the silica arrayed surface displayed an extraordinary superhydrophobicity with a self-cleaning property despite its hydrophilic chemical composition.

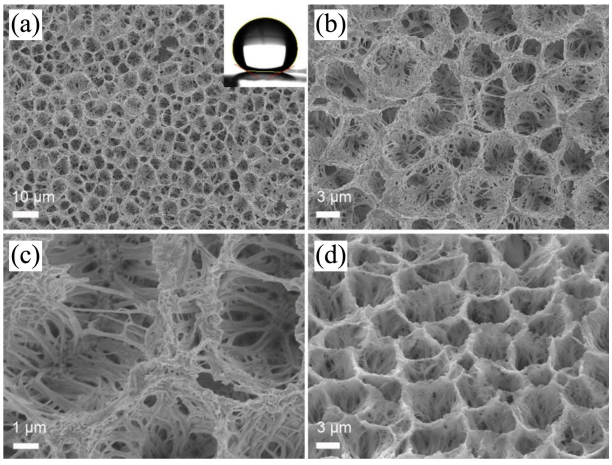

Figure 5. Top-viewed (a-c) and tilted (d) scanning electron micrograph images of the silica microbowl structure at different magnifications. The silica microbowl structure on polydimethylsiloxane (PDMS) was obtained using the alumina template of 20 nm diameter and 12 μm in length, followed by the hydrophobic drying condition. Inset image is the shape of a water drop on the silica microbowl-arrayed structure on PDMS, indicating its superhydrophobic property.

It was previously demonstrated that silica nanostructures remain unchanged after treatment of piranha solution and surface modification with (3-aminopropyl)triethoxysilane.[29] Here, a further experiment was carried out with three different types of silica array structures. The results revealed that the structural morphology did not change with an additional acid treatment, organic solvent washing, or surface immobilization with (3-trimethoxysilylpropyl)-diethylenetriamine after fabrication had been completed, indicating that the SNT-arrayed structure is stable enough to be used for further applications.

Conclusion

We successfully fabricated silica nano- and micro-structures on a PDMS substrate using a silica-coated AAO template. The silica nano- and microbundle structures showed hydrophobic and adhesive properties, caused by increasing the surface area and the hydrophilic interaction with water droplets. The silica microbowl structure exhibited superhydrophobicity with an anti-adhesive force, due to the hierarchical micro/nanostructure. The strategy used in this study provided a superhydrophobic property using hydrophilic silica materials, suggesting that surface geometry had a significant effect on the hydrophobicity of the material. Since SNT arrays provide biocompatibility and a wide range of hydrophobicities capable of being controlled by aspect ratio, the hydrophobic surface composed of SNT array could be an attractive candidate for ideal materials constructing biomedical devices, such as cell and protein chips.

Acknowledgments. This study was supported by the Korea Research Foundation Grant funded by the Korean Government (KRF-2008-313-C00581). This research was supported by the Kyungwon University Research Fund in 2008.

References

1. Wang, S.; Jiang, L. *Adv. Mater.* **2007**, *19*, 3423.

2. Jin, M.; Feng, X.; Feng, L.; Sun, T.; Zhai, J.; Li, T.; Jiang, L. *Adv. Mater.* **2005**, *17*, 1977.
3. Song, X.; Zhai, J.; Wang, Y.; Jiang, L. *J. Phys. Chem. B* **2005**, *109*, 4048.
4. Feng, L.; Li, S.; Li, Y.; Li, H.; Zhang, L.; Zhai, J.; Song, Y.; Liu, B.; Jiang, L.; Zhu, D. *Adv. Mater.* **2002**, *14*, 1857.
5. Sun, T. L.; Feng, L.; Gao, X. F.; Jiang, L. *Acc. Chem. Res*. **2005**, *38*, 644.
6. Feng, L.; Li, S.; Li, H.; Zhai, J.; Song, Y.; Jiang, L.; Zhu, D. *Angew. Chem. Int. Ed*. **2002**, *41*, 1221.
7. Zhang, X.; Shi, F.; Yu, X.; Liu, H.; Fu, Y.; Wang, Z.; Jiang, L.; Li, X. *J. Am. Chem. Soc*. **2004**, *126*, 3064.
8. Oner, D.; McCarthy, T. J. *Langmuir* **2000**, *16*, 7777.
9. Hong, X.; Gao, X.; Jiang, L. *J. Am. Chem. Soc.* **2007**, *129*, 1478.
10. Yim, E. K.; Reano, R. M.; Pang, S. W.; Yee, A. F.; Chen, C. S.; Leong, K. W. *Biomaterials* **2005**, *26*, 5405.
11. Fuard, D.; Tzvetkova-Chevolleau, T.; Decossas, S.; Traqui, P.; Schiavone, P. *Microelec. Eng*. **2008**, *129*, 1289.
12. Feng, X.; Feng, L.; Jin, M.; Zhai, J.; Jiang, L.; Zhu, D. *J. Am. Chem. Soc.* **2004**, *126*, 62.
13. Hosono, E.; Fujihara, S.; Honma, I.; Zhou, H. *J. Am. Chem. Soc*. **2005**, *127*, 13458.
14. Zhang, L.; Wu, J.; Wang, Y.; Long, Y.; Zhao, N.; Xu, J. *J. Am. Chem. Soc.* **2012**, *134*, 9879.
15. Yang, S.; Chen, S.; Tian, Y.; Feng, C.; Chen, L. *Chem. Mater.* **2008**, *20*, 1233.
16. Zha, L.; Cebeci, F. C.; Cohen, R. E.; Rubner, M. F. *Nano Lett*. **2004**, *4*, 1349.
17. Hikita, M.; Tanaka, K.; Nakamura, T.; Kajiyama, T.; Takahara, A. *Langmuir* **2005**, *21*, 7299.
18. Coffinier, Y.; Janel, S.; Addad, A.; Blossey, R.; Gengembre, L.; Payen, E.; Boukherroub, R. *Langmuir* **2007**, *23*, 1608.
19. Niu, J. J.; Wang, J. N. *Cryst. Growth Des*. **2008**, *8*, 2793.
20. Masuda, H.; Fukuda, K. *Science* **1995**, *268*, 1466.
21. Li, A. P.; Muller, F.; Birner, A.; Nielsch, K.; Gosele, U. *J. Appl. Phys*. **1998**, *84*, 6023.
22. Kovtyukhova, N. I.; Mallouk, T. E.; Mayer, T. S. *Adv. Mater.* **2003**, *15*, 780.
23. Son, S. J.; Lee, S. B. *J. Am. Chem. Soc*. **2006**, *128*, 15974.
24. Liddle, J. A.; Cui, Y.; Alivisatos, P. *J. Vac. Sci. Technol. B* **2004**, *22*, 3409.
25. Krachevsky, P. A.; Nagayama, K. *Adv. Colloid Interface Sci*. **2000**, *85*, 145.
26. Shchukarev, A.; Rosenqvist, J.; Sjoberg, S. *J. Elec. Spec. Related Phenomena* **2004**, *137-140*, 171.
27. Huang, X. J.; Kim, D. H.; Im, M.; Lee, J. H.; Yoon, J. B.; Choi, Y. K. *Small* **2009**, *5*, 90.
28. Li, Y.; Li, C.; Cho, S. O.; Duan, G.; Cai, W. *Langmuir* **2007**, *23*, 9802.
29. Kim, S. Y.; Yu, J.; Son, S. J.; Min, J. *Ultramicroscopy* **2010**, *110*, 659.